

Long-Time Correlations and Hydrophobe-Modified Hydrogen-Bonding Dynamics in Hydrophobic Hydration

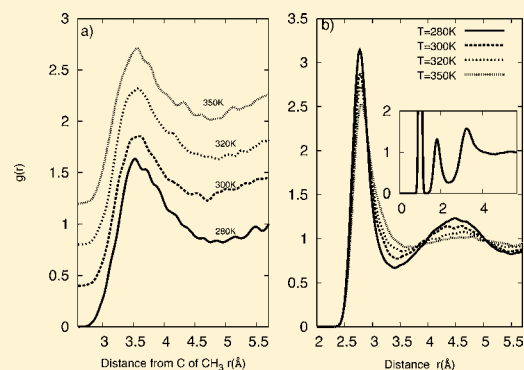
John Tatini Titantah[†] and Mikko Karttunen^{*‡}

[†]Department of Applied Mathematics, The University of Western Ontario, London, Ontario, Canada N6A 5B7

[‡]Department of Chemistry, University of Waterloo, 200 University Avenue West, Waterloo, Ontario, Canada N2L 3G1

S Supporting Information

ABSTRACT: The physical mechanisms behind hydrophobic hydration have been debated for over 65 years. Spectroscopic techniques have the ability to probe the dynamics of water in increasing detail, but many fundamental issues remain controversial. We have performed systematic first-principles *ab initio* Car–Parrinello molecular dynamics simulations over a broad temperature range and provide a detailed microscopic view on the dynamics of hydration water around a hydrophobic molecule, tetramethylurea. Our simulations provide a unifying view and resolve some of the controversies concerning femtosecond-infrared, THz–GHz dielectric relaxation, and nuclear magnetic resonance experiments and classical molecular dynamics simulations. Our computational results are in good quantitative agreement with experiments, and we provide a physical picture of the long-debated “iceberg” model; we show that the slow, long-time component is present within the hydration shell and that molecular jumps and over-coordination play important roles. We show that the structure and dynamics of hydration water around an organic molecule are non-uniform.



INTRODUCTION

“Liquid water is not a ‘bit player’ in the theater of life,” as Martin Chaplin points out. “It’s the headline act.”¹ Possessing numerous anomalous properties, 63 of which are listed by Chaplin as vital to both our everyday life and biological existence, water is unquestionably a complex liquid.^{1–5} Water is not merely a static solvent, but it is fundamental to dynamic processes including protein folding, properties of DNA, the hydration dynamics of small molecules, and even cellular signaling.^{1,6} New exciting experiments by Nucci et al. have also suggested that the dynamics of hydration water around biological molecules is complex and non-uniform and depends on the contact site with the protein.⁷ In addition, recent simulations have provided direct evidence that the dynamics of solvation water is significant in drug docking.⁸ In the crowded cellular environment, hydrogen-bonding (HB) properties between H₂O molecules and their collective dynamics, along with the interactions of clusters of H₂O molecules with hydrophobic groups of biological molecules, are particularly important. This collective effect is referred to as the hydrophobic force or hydrophobic effect.

In 1945, Frank and Evans observed decreased entropy and enthalpy upon mixing water with hydrophobic molecules and suggested that hydrophobic groups enhance ordering of solvation water.⁹ This so-called “iceberg model” remains hotly debated and controversial.^{2,5,10,11,13,14} Direct experimental confirmation of enhanced ordering, or “icebergs”, and whether it occurs or not, is very difficult because both time-averaged and spatially averaged measurements wash away important details

of dynamic behavior. Experiments must not only distinguish between the solvation shell and bulk H₂O molecules but also provide temporal resolution in the femtosecond scale to resolve processes such as translational and librational motion, rapid reorientation, possible jump exchanges of HB partners, and so on.

Spectroscopic techniques provide the most convenient experimental method to probe such properties, as they avoid many of the problems of spatial and temporal averaging. The most direct experimental evidence of the special properties of solvation shell water came from fs-IR spectroscopy experiments by Rezus and Bakker on the OH stretch vibration, which showed a strong reduction in OH rotational motion,¹¹ thus supporting the iceberg hypothesis. This technique has also been used to show that a small fraction of water molecules in the solvation shell of urea, a well-known protein-denaturant, experiences very slow HB dynamics; urea’s cooperation with water in solvating amino acid residues provides a possible mechanism by which urea denatures proteins.¹² Over the past few years, an increasing number of experiments probing solvation properties have emerged.^{13–19} In addition, infrared spectroscopy studies of two biologically relevant molecules, *tert*-butyl alcohol (TBA) and trimethylamine *N*-oxide (TMAO), have revealed that the latter molecule introduces higher coordination in the solvation water than the former.^{20,21} This finding has also been confirmed by Fourier-transform infrared

Received: March 5, 2012

Published: May 14, 2012

(FT-IR) spectroscopy.²² However, OHD-optical Kerr effect measurements carried out on aqueous solutions of urea, formamide, TMAO, and tetramethylurea (TMU) found no signature of immobilized water.²³

While most NMR experiments tend to average out many of the subtle properties, recent experiments by Qvist and Halle¹⁴ provide a serious challenge to the iceberg hypothesis: They suggested that at supercooled temperatures, solvation water becomes less constrained; i.e., it rotates faster than bulk water. They also proposed that there is no difference in HB energy between the solvation shell water molecules and in bulk, and that there is no significant slowing down on hydration water at room temperature, thus contradicting directly the suggestions based on fs-IR measurements.^{11,17}

Computer simulations offer an alternative method and have the advantage of being able to provide direct information about the above properties. One of the earliest classical molecular dynamics (MD) simulations (214 ST2 water molecules) was performed by Zichi and Rossky.²⁴ From a 25 ps trajectory they measured librational frequency modes and found that there is a clear difference between solvation shell and bulk water, and they interpreted their findings as a manifestation of different intermolecular association of water molecules in the first solvation shell and bulk. Another major development came 23 years later when, based on classical 75 ps MD simulations at room temperature, Laage et al.²⁵ claimed, in contrast to fs-IR experiments,^{11,17} that “no water molecules are immobilized by hydrophobic solutes” and that the behavior can be explained by a jump model,²⁶ adding to the controversy. Although classical MD is successful in many occasions, to make quantitative and reliable comparison with the above experiments, quantum mechanical force-field-independent *ab initio* simulations are needed. The quantum mechanical approach has become more common,^{27–31} but until now, comprehensive studies of hydrophobic hydration have been missing.

In this work, we use *ab initio* Car–Parrinello molecular dynamics (CPMD) simulations to systematically investigate the dynamical properties of water molecules around a hydrophobic molecule, TMU, an osmolyte, over a broad temperature range from 270 to 450 K. We chose TMU since it is commonly studied in femtosecond spectroscopy measurements^{11,14,17,32} and simulations²⁵ under similar or comparable conditions. Due to the high computational cost of *ab initio* simulations, we were restricted to only one type of solute molecule. Each simulation run is at least 100 ps, and the total simulation time is ~800 ps. Our results are in quantitative agreement with different experiments, as will be discussed in detail. We resolve many of the controversies and show the microscopic origin of their differences.

METHODS

We used the constant particle number, volume, and temperature (NVT) ensemble to perform quantum mechanical CPMD³³ simulations using the CPMD code.³⁴ Van der Waals interactions were accounted for by using the corrections introduced by Grimme.⁵⁶ Inclusion of van der Waals interactions in *ab initio* simulations, and if and under which conditions that should be done, is currently a very active field of research on its own.^{57,58} Another very active field is the development of new exchange and correlation functionals, hybrid and with softer non-local term (PBE0, optPBE-vdW, and vdW-DF2).^{58,59} This has resulted in ambient water properties that are compatible with measurements on high-density water.³⁶ Other workers have used the self-consistent polarization DFT approach to the dispersion energy to improve upon the binding energies and the harmonic frequencies of

clusters of a few water molecules; the structural properties of the clusters, however, were not greatly improved when compared with BLYP-based DFT calculations.³⁷ Development and testing remain very important.^{59,60}

We used the BLYP functional, as it is one of the most tested and widely used functionals. Direct comparison between the various published results is sometimes not straightforward, as simulation conditions vary from one work to the other.^{38–40} We also performed simulations without the van der Waals corrections⁵⁶ and found the results presented here to be robust and within the margin of error. We chose the canonical (NVT) ensemble since NVE *ab initio* simulations have been reported to produce overstructuring of water: Lee and Tuckerman³⁵ performed a comparative study of different protocols and recommend using NVT. Importantly, our radial distribution functions for neat water are in good agreement with the experiments of Soper.³⁶ Periodic boundary conditions were applied, and a Nosé–Hoover chain thermostat⁴¹ was used to keep the temperature constant. Temperature was varied between 270 and 450 K. This was done by subjecting a pre-equilibrated liquid (at 300 K) to each of the temperatures. Becke–Lee–Yang–Parr gradient corrections to the exchange and correlation energy^{42,43} were applied, and the Troulier–Martins pseudopotentials (PPs) for oxygen, carbon, and nitrogen⁴⁴ and the Kleinman–Bylander PP⁴⁵ for hydrogen were used. The plane-wave basis set for the valence states was given up to a cutoff of 80 Ry. The simulation cell was chosen to be cubic. A time step of 5 au (~0.121 fs) was used, while the electrons were given a fictitious mass of 400 au. The simulations of neat water were done on a system of 54 H₂O molecules, while the simulations with one TMU had 50 H₂O molecules. As a control, we also simulated a system of 105 H₂O molecules at room temperature. This control system demonstrates that the results obtained using the smaller system size of 50 H₂O+1TMU molecules are reliable, as the pair correlation functions, solvation shell structure, and OH orientation correlation function (OCF) agree well between the two systems of different sizes (see Supporting Information for a detailed comparison). All systems were kept at a constant density of about 1 g/cm³, and all calculations were done at the Γ -point of the Brillouin zone. Ewald summation was used for the long-range Coulomb interactions. Excellent accounts of *ab initio* simulations of aqueous systems are provided, e.g., by Marx et al.^{34,46}

The structure was first energy-minimized, and then the wave function of each system was converged by energy minimization using the conjugate gradient method, where convergence was attained when the largest value of the gradient of the wave function was $<10^{-6}$. This was followed by a 50 ps equilibration run and a 50 ps production run. The averages and correlation functions were computed for time windows of varying size and origin to ensure that sampling was adequate and non-correlated (autocorrelation functions provided the relevant time scales) and that convergence was reached.

RESULTS

Structure of Solvation Water. We start our analysis from the O–O pair correlation functions ($g(r)$) for water. As a reference, we measured the O–O and O–H partial pair correlation functions for neat water and found them to be in good quantitative agreement (see right panel of Figure 1) with experiments of Soper.³⁶ The O–O first-neighbor distance of 2.79 Å is also in very good agreement with X-ray diffraction value of 2.83 Å and neutron scattering value of 2.75 Å (see ref 27 and references therein). It should be noticed, however, that while neutron scattering is good for studying the properties of neat water, it cannot resolve the detailed structures of hydration shells around a hydrophobic molecule the same way as spectroscopic methods can, since neutron scattering provides a spatially averaged quantity. The effect of the inclusion of van der Waals corrections on the pair correlation function is very small. The O–O first-neighbor distance of 2.79 Å remains unchanged. The first minimum in the $g(r)$ passes from a

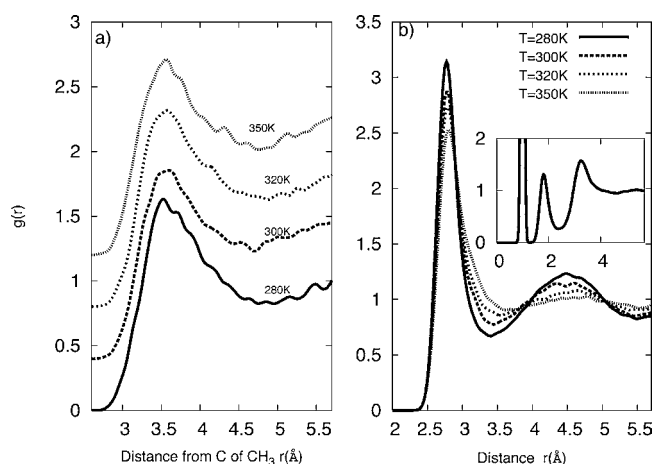


Figure 1. (a) Time-averaged water density as a function of the distance from the carbon atom of the CH_3 group of the TMU molecule ($g(r)$) for temperatures in the range 280–350 K. Curves have been shifted for clarity. (b) O–O pair correlation functions for TMU–water solution. The inset shows the O–H $g(r)$ for neat water. This is in good agreement with experiments of Soper.³⁶

distance of 3.3–3.4 Å. The height of the first nearest-neighbor peak of ~ 2.9 at 300 K increases slightly to 3.0, while the depth of the first minimum decreases from 0.79 to 0.73 without the van der Waals correction. The slight overstructuring is less than reported by other workers using PBE exchange and correlation functionals.³⁸

Next, we computed $g(r)$ with respect to the carbon atoms of the CH_3 groups of the TMU molecule (left panel of Figure 1). This figure suggests that the first solvation shell of water extends from a distance of ~ 2.8 to ~ 5 Å from the carbon atom of the CH_3 group and that in this shell water organizes into broad strata around the CH_3 groups. The latter is a direct indication of a non-uniformity of the dynamics of solvation water around TMU⁷ and may explain the fs-IR observation that each methyl group only slows down the rotational motion of four OH groups.¹¹ We will discuss the origin of this observation later in connection with the dynamics of water. The solvation shell range obtained here is in agreement with previous theoretical work which shows a similar range for water solvating non-polar centers of a protein molecule.⁴⁷

Hydrogen-Bonding (HB). Next, we explored the temperature dependence of HB relaxation by calculating the correlation functions for the number of HBs per water molecule $C_{\text{HBN}}(t)$ and for the hydrogen bond length $C_{\text{HBL}}(t)$

$$C_{\text{HBN}}(t) = \frac{\langle \Delta n_{\text{HB}}(t) \Delta n_{\text{HB}}(0) \rangle_0}{\langle (\Delta n_{\text{HB}}(0))^2 \rangle_0},$$

$$C_{\text{HBL}}(t) = \frac{\langle \Delta r_{\text{HB}}(t) \Delta r_{\text{HB}}(0) \rangle_0}{\langle (\Delta r_{\text{HB}}(0))^2 \rangle_0} \quad (1)$$

where $n_{\text{HB}}(t)$ is the instantaneous number of HBs per H_2O and r_{HB} is the hydrogen bond length, defined as the distance between the oxygen atom of the HB accepting water and the hydrogen atom donating the HB. A similar correlation function is calculated for the distance between the oxygen atoms of the hydrogen-bonded water pairs $\text{C}_{\text{O-O}}$. Two water molecules are considered to be hydrogen-bonded when the distance between their oxygen atoms is < 3.3 Å (corresponding to the first minimum in the O–O partial pair correlation function of water, as the right panel of Figure 1 shows), and the angle between the

vector joining the two oxygen atoms and the OH bond of the HB-donating water molecule is $< 30^\circ$.

The results are shown in Figure 2a. We also performed similar calculations for HB relaxation in neat water and, in

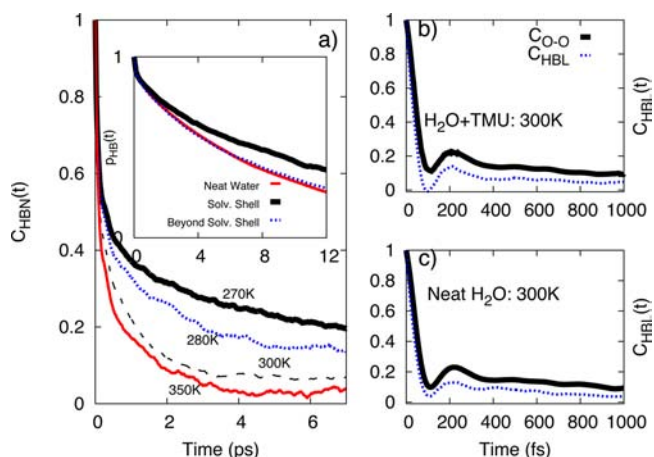


Figure 2. (a) Hydrogen bond population correlation function $C_{\text{HBN}}(t)$ at various temperatures with TMU present. (b,c) O–O distance correlation functions at $T = 300$ K for water and TMU, and for neat water, respectively. The inset in panel (a) shows the probability (at 300 K) that a pair of water molecules remains hydrogen-bonded after time t , after forming a HB at $t = 0$ (eq 2).

contrast to the case with TMU present, no long-time component was observed at any temperature. In the system with no TMU present, a biexponential fit at $T = 300$ K provided time scales of about 80 fs and 1.4 ps (see Supporting Information for fitting details). The former corresponds to the high frequency librational HB exchange.^{10,49} However, as we will show later, this time scale is also present in large-angle molecular jumps that the water molecules perform. The latter time scale is the regular HB breaking by reorientation, as reported in virtually all the experiments cited here.

When a TMU molecule is present, a similar biexponential fit yielded times of 200 ± 50 fs and 12 ± 4 ps. To examine the quality of the fit, we measured the root-mean-square residue (RMSR). For pure water, the value was found to be 0.013. When TMU was present it increased by more than a factor of 6 to 0.083: A biexponential fit is not sufficient to accurately model HB dynamics in the solvation shell of the TMU molecule. We then considered a triexponential fit, which yielded the following time scales: 55 ± 10 fs, 0.7 ± 0.1 ps, and 16 ± 3 ps. RMSR decreased to 0.014 (see Figure S2 of Supporting Information for details). The third time scale shows that there is a drastic increase in the HB lifetime in the solvation shell of the TMU molecule.

An effective collective HB correlation time can be defined as the integral of the correlation function. Such analysis shows that HBs in the solvation shell of TMU live 5 times longer than those in bulk water. This slowing down in HB dynamics is of the same order as the finding of Bakker, who found 6 times slower dynamics for water solvating BF_4^- than bulk water,⁴⁸ and others who found slowing down by a factor of 3–10, depending on concentration of TMU solution.^{17,52} Analysis based on C_{HBN} alone is not enough to identify the origin of the faster time scale. We will discuss this again in connection with large-angle jumps, where the microscopic processes can be

identified. The observed long time scale is in excellent agreement with fs-IR experiments performed under the same conditions (concentration and temperature) on water-solvating TMU^{11,17} and is due to the slow dynamics of the solvation shell HBs. This slowing down of solvation water has been a highly controversial issue, with fs-IR and NMR results suggesting almost opposite behaviors.^{11,14,17} Our further analysis resolves this controversy. Before we discuss this in more detail, we would like to point out that we also evaluated the probability that a HB formed between a pair of water molecules remains intact after time t . This was done by calculating the correlation of $h(t)$, where $h = 1$ when the bond remains intact from time $t = 0$ until time t , and $h = 0$ otherwise.

$$p_{\text{HB}}(t) = \frac{\langle h(0)h(t) \rangle_0}{\langle (h(0))^2 \rangle_0} \quad (2)$$

The results of these calculations also revealed (inset in Figure 2a) that HBs in the solvation shell of TMU have a longer life-span than those in the bulk.

OH Stretch Frequency Correlation Function. To gain more insight into HB dynamics and to compare with fs-IR experiments, we measured the OH stretch frequency correlation function. fs-IR spectroscopy allows for probing of relaxation times within water down to sub-50 fs time scales.^{10,15,50} The OH vibrational frequency $\omega_{\text{OH}} = 1/\tau(t)$ of H₂O molecules can be obtained by maximizing the function⁵¹

$$F(t, \tau) = \left| \frac{1}{\sigma\sqrt{2\pi\tau}} \int_{-\infty}^{+\infty} ds f(s) e^{2\pi i(s-t)/\tau} e^{-(s-t)^2/2\tau^2\sigma^2} \right|^2 \quad (3)$$

with respect to τ . f is the instantaneous length of the OH bond whose frequency is probed. The two OH bonds in H₂O are examined independently. The Gaussian weight ensures localization of the wave package for a segment of time centered at t . Smooth frequency variation with time and adequate localization are ensured by setting $\sigma = 2$.

With the time dependence of these frequencies determined, we calculated the frequency correlation function

$$C_{\omega_{\text{OH}}}(t) = \frac{\langle (\omega(t) - \langle \omega \rangle)(\omega(0) - \langle \omega \rangle) \rangle}{\langle (\omega(0) - \langle \omega \rangle)^2 \rangle} \quad (4)$$

Averaging is over the initial times $t = 0$ and the OH groups.

We first measured relaxation of OH frequency in neat water. At $T = 300$ K, a biexponential fit of the calculated $C_{\omega_{\text{OH}}}$ (figure not shown) gave time scales of ~ 82 fs and ~ 1.5 ps, corresponding well with the results for C_{HBN} . The fast time scale was found to be practically temperature-independent, whereas the latter was sensitive to temperature. We speculate that at least part of the contribution to the fast, temperature-independent time scale is from the resonant intermolecular energy transfer time of 80 fs found by Kraemer et al.¹⁵ This fast relaxation is due to underdamped HB oscillations, which account for the peak at 168 fs found in our simulated frequency–frequency correlation. This value is in excellent agreement with the vibrational echo peak shift value of 170 fs obtained by Fecko et al.¹⁰ The longer time scale corresponds to the average HB lifetime.

Introduction of TMU leads to three time scales: a fast relaxation time of 70 ± 10 fs, which is almost temperature-independent as above, a temperature-dependent bulk water relaxation time $\tau_2^{\text{OH}} \approx 1$ ps, and a very long time process (>10 ps), whose contribution increases with decreasing temperature.

This latter time is of the same order as the longest time scale in the collective HB relaxation, demonstrating the direct correlation between the HB dynamics and the OH stretch frequency. We also observed that $>50\%$ of the water OH frequency relaxation occurs within about 50 fs, which is in perfect agreement with vibrational echo peak shift measurement of the OH stretch vibration of HOD in D₂O.¹⁰

We also computed similar correlation functions separately for O–O and OH \cdots O distances for water molecules. Figure 2b,c shows the rapid decay time of 80 fs as described above and a bump at about 210 fs followed by a decay. Those features are present at all temperatures in neat water as well as in the presence of TMU. Fecko et al. also measured the O–O distance correlation in neat water (low concentration of non-interacting OH oscillators),¹⁰ and their results are in quantitative agreement with ours. As the two figures show, the OH \cdots O correlation decays almost to zero within 80 fs in a solution with TMU present, while that of O–O remains practically the same as that of neat water. This is an indication of hydrophobe-modified HB dynamics in the solvation shell.

Orientation Correlation Functions. In addition to OH stretching, water molecules rotate, and there has been a lot of controversy related to slowing down of rotations and its importance in solvation water when hydrophobic molecules are present.^{11,14,26} It is generally agreed that some slowing down exists, but whether or not that is significant, and if some of the water molecules become immobilized close to hydrophobic groups, remains highly debated.^{2,14,17,25} We monitored rotational dynamics by measuring the OH orientation vector correlation function $C_n(t) = \langle P_n(\cos \theta(t)) \rangle$, where P_n is the Legendre polynomial of order n and $\theta(t)$ is the angle the OH vector will sweep through in time t . We calculated C_n for $n = 2$. The results are shown in Figure 3a. A long-time component is

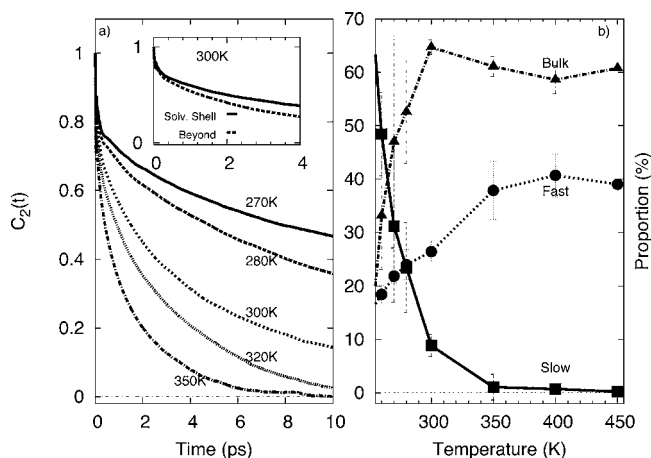


Figure 3. (a) OH orientation correlation function $C_2(t)$ as function of temperature and time. The inset shows C_2 for water molecules in the solvation shell (Solv. Shell) and outside the solvation shell (Beyond) of the TMU molecule at $T = 300$ K. (b) Three time scales are present (from $C_2(t)$): fast $\tau_{\text{rot}}^{\text{fast}}$, bulk $\tau_{\text{rot}}^{\text{bulk}}$ and slow $\tau_{\text{rot}}^{\text{slow}}$. The proportions of these components vary with temperature.

clearly present. We found that a sum of three exponential functions was required to correctly model this correlation. At room temperature, the corresponding correlation times are a fast time of about 80 ± 10 fs (denoted τ_1^{rot}), a bulk-like time of about 3.1 ps (denoted τ_2^{rot}), and a slow rotational time (>10 ps)

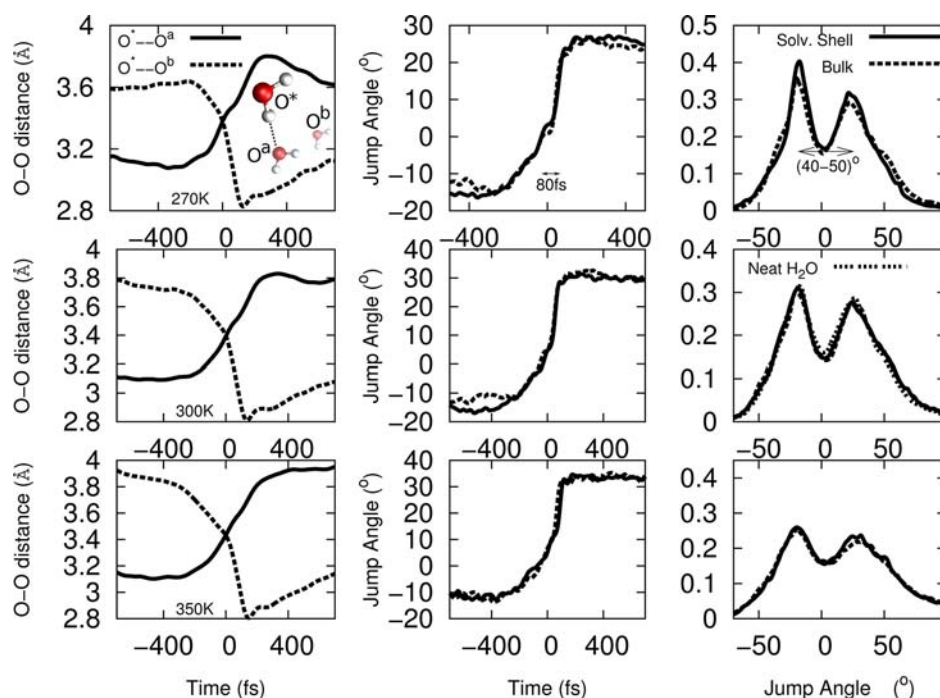


Figure 4. Left: Time dependence of the O^*-O^a and O^*-O^b distances between central rotating water molecule O^* hydrogen-bonded to water molecule O^a before HB cleavage (at $t = 0$) to form a HB with the water molecule O^b at $T = 270$ (top), 300 (middle), and 350 K (bottom). The inset shows O^* , O^a , O^b , and the H-bond before cleavage. Middle: Time dependence of the jump angle in the solvation shell (Solv. Shell) and in bulk. Right: Jump angle distribution for water molecules in solvation shell and in bulk. The large-angle jump of $49^\circ \pm 4^\circ$ recently reported for HB exchange in aqueous perchlorate solution using polarization-selective multidimensional vibrational spectroscopy¹³ is also found in this work ($45^\circ \pm 5^\circ$).

denoted $\tau_{\text{slow}}^{\text{rot}}$, which is only present for the water–TMU system and not for bulk water.

We analyzed C_2 in more detail and resolved the proportions in which the fast (τ_1^{rot}), bulk (τ_2^{rot}), and slow ($\tau_{\text{slow}}^{\text{rot}}$) time scales are present at different temperatures. As the figure shows, below $T = 350$ K the slow component starts to increase as the temperature is lowered, and around $T = 300$ K about 10% of H_2O molecules are “slow”. In neat water no slow component is present at 300 K. If we compare this to the pair correlation functions in Figure 1, we can say that not all the water molecules in the solvation shell (~ 14) are slow, but only about 5 molecules ($\sim 10\%$ of all molecules) are slowed down. This number matches well with fs-IR measurements.^{11,17} This slow decay in Figure 3a is very similar to the fs-IR measurements of Rezus and Bakker.¹¹ This strong slowing down has been seriously challenged by the classical MD simulations of Laage and Hynes^{25,26} and NMR experiments by Qvist and Halle,¹⁴ but our parameter-free simulations show that it is clearly present and that the proportion of slow molecules is highly temperature dependent.

Petersen et al. used fs-IR to obtain rotational activation energies of 17 ± 1 kJ/mol for bulk water and 29 ± 3 kJ/mol for solvation water.⁵² Tielrooij et al. used GHz–THz dielectric relaxation and obtained slightly lower values of 12 and 22 kJ/mol for bulk and solvation water, respectively.¹⁷ We used the temperature dependence of the OCF relaxation time τ_2^{rot} to extract activation energies for neat water and water in TMU–water solution. Above 270 K, we obtained 22–24 kJ/mol for solvation water and 16 ± 2 kJ/mol for neat water. Both results are in perfect accord with the GHz–THz dielectric relaxation results.¹⁷

Molecular Jumps. Water molecules oscillate and rotate, and Laage and Hynes^{25,26} suggested that HBs break and reform by a jump mechanism mediated by defect states:^{25,26} a water molecule forms five H-bonds and an unstable transition state comprising a bifurcated H-bond. This water molecule then undergoes a large-amplitude (~ 60 – 70°) jump within a time frame of ~ 0.2 ps. Using classical MD simulations, they suggested that the slowing down in water dynamics near the hydrophobic group observed in fs-IR¹¹ is only minor and the excluded volume effects close to the solute dominate the behavior.²⁵ This interpretation is in direct contrast to Bakker et al.,^{11,17} who claimed a significant slowing down of water close to hydrophobic molecules. As discussed above, our findings support Bakker et al.,¹¹ and we see clear slowing down. The molecular jumps and the five coordinated defect states as suggested by Laage and Hynes^{25,26} were, however, present as we will discuss below.

We investigated the evolution of HB coordination and the involved microscopic mechanisms. We use the same notation as Laage and Hynes²⁶ and identify three H_2O molecules: O^* denotes the rotating water molecule; O^a is the water molecule accepting an HB from O^* before the jump; O^b stands for the water molecule that will form an HB with O^* after the jump. The origin of time is set at $t = 0$ when the O^*-O^a and O^*-O^b distances are equal. In addition to the HB coordination, we also calculated the $OH \cdots O$ HB distance between the H atom of the rotating OH group and the HB-accepting oxygen atom before and after the OH jump. As the left panel of Figure 4 shows, the time dependence of both distances is very similar to that reported by Laage and Hynes.²⁶ A comparison with pair correlation data shows that all distances are close to the first minimum in the O–O pair correlation, which indicates that

over-coordination and defects caused by a complex and highly fluctuating HB network may be responsible for the observed anomalies.

The middle panels of Figure 4 show the time evolution of the jump angles in the solvation shell, beyond it, and also in neat water (separate simulation) at different temperatures just before ($t < 0$) and after ($t > 0$) the OH jumps. In agreement with Laage et al.,²⁵ we find not only that solvation water molecules perform jumps, but that the jumps are very similar to those in bulk water. We find a jump angle value of $45 \pm 5^\circ$, which is similar to the experimentally observed value of $49 \pm 4^\circ$ reported by Ji et al. for HB exchange in aqueous perchlorate solution using polarization-selective multidimensional vibrational spectroscopy,¹³ but $15\text{--}25^\circ$ smaller than suggested by the classical MD simulations.²⁶

A detailed analysis shows that each rapid jump is preceded by a slow (sub-picosecond) angular reorientation until $\theta = 0$, from which the OH group undergoes a large-angle rapid flip. This flip occurs in ~ 80 fs (Figure 5). This time is found to be the

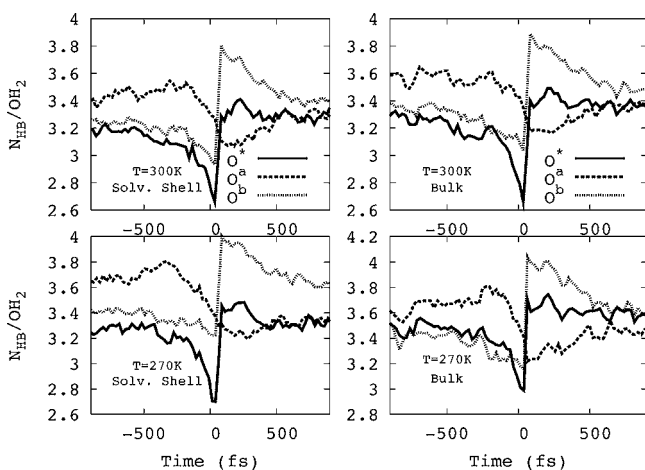


Figure 5. Jump coordinations for bulk and solvation water at $T = 270$ and 300 K. Notations follow Laage and Hynes:²⁶ O^* is the rotating water molecule, O^a is the water molecule accepting an HB from the rotating water molecule, and O^b is the molecule that will replace O^a after O^* undergoes the jump. The time $t = 0$ corresponds to the instant when the $O^* - O^a$ and $O^* - O^b$ distances are equal.

same in the solvation shell, bulk, and neat water and is independent of temperature. It is the same as that found in this work for rapid OH stretch frequency and the fast HB population correlation time, and it is in perfect agreement with fs-IR spectroscopy measurements,^{11,15,53} where this time, referred to as intermolecular energy-transfer time,⁵⁴ was found to be temperature-insensitive.¹⁵

To get an even more microscopic picture, we analyzed O^* , O^a , and O^b triplets as described above. Figure 5 shows the number of HBs around the water molecules before and after the jump. It is clear that O^a always has a larger number of HBs as compared to O^* and O^b before the jump, but O^b becomes over-coordinated after the jump. The jump process is characterized by three events: reorientation, a rapid jump together with an instantaneous increase in coordination (O^* and O^b), and a slow decrease in the HB population around O^a , as clearly shown in Figure 5. Importantly, the rapid librations (fluctuations in Figure 5) and the rapid jump (O^*) occur on the same time scale (~ 80 fs). The time scale in which O^* loses HBs before the jump is ~ 200 fs (the decay in HB coordination

before the jump). In addition, this decay is accompanied by an increase in the HB coordination of O^a . After the jump, O^b becomes highly coordinated and slowly decays toward its equilibrium value.

Let us compare the above with experiments and the framework set by Laage and Hynes.^{25,26} The microscopic picture that emerges from our simulations agrees with Laage and Hynes in the sense that there are rapid jumps and that over-coordinated water has a crucial role. The jump angles we see are, however, smaller and match perfectly with the experiments of Ji et al.¹³ We analyzed *all* jump events and did not observe concerted jumps, as suggested by Laage and Hynes²⁶ based on their classical MD simulations. The process is collective in the sense that it involves several (at least three) molecules at the same time and apparent immediate reorganization of the HB network, but no concerted jumps were observed. The long time scale seen in spectroscopic experiments^{11,17,52} and in the correlation functions here cannot be explained with switching off of the jumps:⁵⁵ we analyzed all individual jumps, and they are always present in roughly the same proportions both in bulk and in solvation water. Further analysis showed that the water molecules closest to the hydrophobic groups show pronounced anisotropy as they orient their dipole moments almost tangentially with respect to hydrophobic groups. Some of these innermost molecules did not leave the solvation shell during the simulations, but they did experience rotations at all temperatures.

DISCUSSION

Based on the above results, we can conclusively say that the observed slowing down and the related long time scale component as reported for water solvating hydrophobic molecules^{11,15,14,17,53} are present. Comparison of correlation functions (Figure 2) revealed that the presence of a hydrophobe modifies HB dynamics, which is manifested as the appearance of a long-time component for solvation shell water. Molecular jumps and over-coordinated bulk water contribute to the difference between HB dynamics in the solvation shell and bulk.

We have refined and provided the full microscopic picture of the jump mechanism suggested originally by Laage and Hynes,²⁶ shown how the molecules involved in HB exchange exhibit different time scales, and identified their origins. The first-principles simulations performed here show where the differences and controversies between various experiments and interpretations emerge and consolidate the view. Finally, our results show that the water molecules in the hydration shell show very different dynamical behaviors. Our detailed analysis showed that a small number of water molecules remain in the hydration shell during the whole simulation time at all temperatures up to 350 K. This non-uniformity is reflected in the long-time tails of the autocorrelation functions and the raggedness of the pair correlation functions, and is in qualitative agreement with the measurements of Nucci et al.⁷ The slow relaxation is the likely cause of the inhomogeneities observed in the pair correlation function in Figure 1.

ASSOCIATED CONTENT

Supporting Information

Discussion about the adequacy of the system size, hydrogen bond relaxation times for solvation and bulk water, and a snapshot from a simulation of the system. This material is available free of charge via the Internet at <http://pubs.acs.org>.

■ AUTHOR INFORMATION

Corresponding Author

mikko.karttunen@uwaterloo.ca

Notes

The authors declare no competing financial interest.

■ ACKNOWLEDGMENTS

M.K. thanks Davide Donadio for helpful discussions. This work has been supported by the Natural Sciences and Engineering Research Council of Canada (M.K.) and SharcNet [www.sharcnet.ca].

■ REFERENCES

- (1) Chaplin, M. *Nat. Rev. Mol. Cell Biol.* **2006**, *7*, 861–866.
- (2) Skinner, J. L. *Science* **2010**, *328*, 985–986.
- (3) Stanley, H. E.; Buldyrev, S. V.; Franzese, G.; Kumar, P.; Mallamace, F.; Mazza, M. G.; Stokely, K.; Xu, L. *J. Phys.: Condens. Matter* **2010**, *22*, 284101.
- (4) Ball, P. *ChemPhysChem* **2008**, *9*, 2677–2685.
- (5) Hilser, V. J. *Nature* **2011**, *469*, 166–167.
- (6) Pal, S. K.; Zewail, A. H. *Chem. Rev.* **2004**, *104*, 2099–123.
- (7) Nucci, N. V.; Pometun, M. S.; Wand, A. J. *Nat. Struct. Mol. Biol.* **2011**, *18*, 245–9.
- (8) Kaszuba, K.; Róg, T.; Bryl, K.; Vattulainen, I.; Karttunen, M. J. *Phys. Chem. B* **2010**, *114*, 8374–86.
- (9) Frank, H. S.; Evans, M. W. *J. Chem. Phys.* **1945**, *13*, 507–532.
- (10) Fecko, C. J.; Eaves, J. D.; Loparo, J. J.; Tokmakoff, A.; Geissler, P. L. *Science* **2003**, *301*, 1698–702.
- (11) Rezus, Y.; Bakker, H. J. *Phys. Rev. Lett.* **2007**, *99*, 148301.
- (12) Rezus, Y.; Bakker, H. J. *Proc. Natl. Acad. Sci. U.S.A.* **2006**, *103*, 18417–18420.
- (13) Ji, M. B.; Odelius, M.; Gaffney, K. J. *Science* **2010**, *328*, 1003–1005.
- (14) Qvist, J.; Halle, B. *J. Am. Chem. Soc.* **2008**, *130*, 10345–53.
- (15) Kraemer, D.; Cowan, M. L.; Paarmann, A.; Huse, N.; Nibbering, E. T. J.; Elsaesser, T.; Miller, R. J. D. *Proc. Natl. Acad. Sci. U.S.A.* **2008**, *105*, 437–42.
- (16) Tielrooij, K. J.; Garcia-Araez, N.; Bonn, M.; Bakker, H. J. *Science* **2010**, *328*, 1006–1009.
- (17) Tielrooij, K.-J.; Hunger, J.; Buchner, R.; Bonn, M.; Bakker, H. J. *Am. Chem. Soc.* **2010**, *132*, 15671–8.
- (18) Soper, A. K.; Teixeira, J.; Head-Gordon, T. *Proc. Natl. Acad. Sci. U.S.A.* **2010**, *107*, E44.
- (19) Huang, C.; et al. *Proc. Natl. Acad. Sci. U.S.A.* **2009**, *106*, 15214–8.
- (20) Freda, M.; Onori, G.; Santucci, A. *J. Phys. Chem. B* **2001**, *105*, 12714–12718.
- (21) Di Michele, A.; Freda, M.; Onori, G.; Santucci, A. *J. Phys. Chem. A* **2004**, *108*, 6145–6150.
- (22) Panuszko, A.; Bruzdziak, P.; Zielkiewicz, J.; Wyrzykowski, D.; Stangret, J. *J. Phys. Chem. B* **2009**, *113*, 14797–14809.
- (23) Mazur, K.; Heisler, I. A.; Meech, S. R. *J. Phys. Chem. B* **2011**, *115*, 2563–2573.
- (24) Zichi, D. A.; Rossky, P. J. *J. Chem. Phys.* **1986**, *84*, 2814–2822.
- (25) Laage, D.; Stirnemann, G.; Hynes, J. T. *J. Phys. Chem. B* **2009**, *113*, 2428–35.
- (26) Laage, D.; Hynes, J. T. *Science* **2006**, *311*, 832–835.
- (27) Kuo, I. F. W.; Mundy, C. J.; McGrath, M. J.; Siepmann, J. I. *J. Chem. Theory Comput.* **2006**, *2*, 1274–1281.
- (28) Mathias, G.; Marx, D. *Proc. Natl. Acad. Sci. U.S.A.* **2007**, *104*, 6980–5.
- (29) Mallik, B. S.; Semparathi, A.; Chandra, A. *J. Phys. Chem. A* **2008**, *112*, 5104–12.
- (30) Sharma, M.; Resta, R.; Car, R. *Phys. Rev. Lett.* **2005**, *95*, 1–4.
- (31) Silvestrelli, P. L. *J. Phys. Chem. B* **2009**, *113*, 10728–10731.
- (32) Bakulin, A. A.; Pshenichnikov, M. S.; Bakker, H. J.; Peteresen, C. *J. Phys. Chem. A* **2011**, *115*, 1821–1829.
- (33) Car, R.; Parrinello, M. *Phys. Rev. Lett.* **1985**, *55*, 2471–2474.
- (34) Marx, D.; Hutter, J. *Ab Initio Molecular Dynamics*; Cambridge University Press: Cambridge, UK, 2009.
- (35) Lee, H.-S.; Tuckerman, M. E. *J. Chem. Phys.* **2006**, *125*.
- (36) Soper, A. K. *Chem. Phys.* **2000**, *258*, 121–137.
- (37) Murdachaew, G.; Mundy, J.; Schenter, G. K. *J. Chem. Phys.* **2009**, *132*, 164102.
- (38) Schwegler, E.; Grossman, J. C.; Gygi, F.; Galli, G. *J. Chem. Phys.* **2004**, *121*, 5400–5409.
- (39) Kuo, I. F. W.; Mundy, C. J.; McGrath, M. J.; Siepmann, J. I.; VandeVondele, J.; Sprik, M.; Hutter, J.; Chen, B.; Klein, M. L.; Mohamed, F.; Krack, M.; Parrinello, M. *J. Phys. Chem.* **2004**, *108*, 12990–1998.
- (40) Jonchiere, R.; Seitsonen, A. P.; Ferlat, G.; Saitta, A. M.; Vuilleumier, R. *J. Chem. Phys.* **2004**, *120*, 300–310.
- (41) Martyna, G. J.; Klein, M. L.; Tuckerman, M. *J. Chem. Phys.* **1992**, *97*, 2635–2643.
- (42) Becke, A. D. *Phys. Rev. A* **1988**, *38*, 3098–3100.
- (43) Lee, C.; Yang, W.; Parr, R. G. *Phys. Rev. B* **1988**, *37*, 785–789.
- (44) Troullier, N.; Martins, J. L. *Phys. Rev. B* **1991**, *43*, 1993–2006.
- (45) Kleinman, L.; Bylander, D. M. *Phys. Rev. Lett.* **1982**, *48*, 1425–1428.
- (46) Marx, D.; Chandra, A.; Tuckerman, M. E. *Chem. Rev.* **2010**, *110*, 2174–2216.
- (47) Bizzarri, A. R.; Cannistraro, S. *J. Phys. Chem. B* **2002**, *106*, 6617–6633.
- (48) Bakker, H. *Nature Chem.* **2009**, *1*, 24–25.
- (49) Luzar, A.; Chandler, D. *Phys. Rev. Lett.* **1996**, *76*, 928–931.
- (50) Loparo, J. J.; Fecko, C. J.; Eaves, J. D.; Roberts, S. T.; Tokmakoff, A. *Phys. Rev. B* **2004**, *70*, 180201.
- (51) Vela-Arevalo, L. V.; Wiggins, S. *Int. J. Bifurc. Chaos Appl. Sci. Eng.* **2001**, *11*, 1359–1380.
- (52) Petersen, C.; Tielrooij, K.-J.; Bakker, H. J. *J. Chem. Phys.* **2009**, *130*, 214511.
- (53) Stenger, J.; Madsen, D.; Hamm, P.; Nibbering, E. T. J.; Elsaesser, T. *Phys. Rev. Lett.* **2001**, *87*, 27401.
- (54) Woutersen, S.; Bakker, H. J. *Nature* **1999**, *402*, 507–509.
- (55) Bakulin, A. A.; Liang, C.; la Cour Jansen, T.; Wiersma, D. A.; Bakker, H. J.; Pshenichnikov, M. S. *Acc. Chem. Res.* **2009**, *42*, 1229–38.
- (56) Grimme, S. *J. Comput. Chem.* **2004**, *25*, 1463–1473.
- (57) Lin, I. C.; Seitsonen, A. P.; Coutinho-Neto, M. D.; Tavernelli, I.; Röhrlisberger, U. *J. Phys. Chem. B* **2009**, *113*, 1127–1131.
- (58) Møgelhøj, A.; Kelkkanen, A. K.; Wikfeldt, K. T.; Schiøtz, J.; Mortensen, J. J.; Pettersson, L. G. M.; Lundqvist, B. I.; Jacobsen, K. W.; Nilsson, A.; Nørskov, J. K. *J. Phys. Chem. B* **2011**, *115*, 14149–14160.
- (59) Zhang, C.; Donadio, D.; Gygi, F.; Galli, G. *J. Chem. Theory Comput.* **2011**, *7*, 1443–1440.
- (60) Kühne, T. D.; Krack, M.; Parrinello, M. *J. Chem. Theory Comput.* **2009**, *5*, 235–241.